https://doi.org/10.1093/brain/awac181 BRAIN 2022: 145; 3594–3607 | 3594

BRAIN
ORIGINAL ARTICLE

Autosomal dominant and sporadic late onset Alzheimer's disease share a common *in vivo* pathophysiology

John C. Morris,[1] Michael Weiner,[2] Chengjie Xiong,[3] Laurel Beckett,[4] Dean Coble,[3] Naomi Saito,[4] Paul S. Aisen,[5] Ricardo Allegri,[6] Tammie L. S. Benzinger,[7] Sarah B. Berman,[8] Nigel J. Cairns,[9] Maria C. Carrillo,[10] Helena C. Chui,[5] Jasmeer P. Chhatwal,[11] Carlos Cruchaga,[12] Anne M. Fagan,[1] Martin Farlow,[13] Nick C. Fox,[14] Bernardino Ghetti,[15] Alison M. Goate,[16] Brian A. Gordon,[7] Neill Graff-Radford,[17] Gregory S. Day,[17] Jason Hassenstab,[1] Takeshi Ikeuchi,[18] Clifford R. Jack Jr,[19] William J. Jagust,[20] Mathias Jucker,[21,22] Johannes Levin,[23] Parinaz Massoumzadeh,[7] Colin L. Masters,[24] Ralph Martins,[25] Eric McDade,[1] Hiroshi Mori,[26] James M. Noble,[27] Ronald C. Petersen,[28] John M. Ringman,[5] Stephen Salloway,[29] Andrew J. Saykin,[30] Peter R. Schofield,[31] Leslie M. Shaw,[32] Arthur W. Toga,[33] John Q. Trojanowski,[34,†] Jonathan Vöglein,[35] Stacie Weninger,[36] Randall J. Bateman[1] and Virginia D. Buckles[1] on behalf of the Dominantly Inherited Alzheimer Network and the Alzheimer's Disease Neuroimaging and Initiative

[†]Deceased.

The extent to which the pathophysiology of autosomal dominant Alzheimer's disease corresponds to the pathophysiology of 'sporadic' late onset Alzheimer's disease is unknown, thus limiting the extrapolation of study findings and clinical trial results in autosomal dominant Alzheimer's disease to late onset Alzheimer's disease.

We compared brain MRI and amyloid PET data, as well as CSF concentrations of amyloid-β_{42}, amyloid-β_{40}, tau and tau phosphorylated at position 181, in 292 carriers of pathogenic variants for Alzheimer's disease from the Dominantly Inherited Alzheimer Network, with corresponding data from 559 participants from the Alzheimer's Disease Neuroimaging Initiative. Imaging data and CSF samples were reprocessed as appropriate to guarantee uniform pipelines and assays. Data analyses yielded rates of change before and after symptomatic onset of Alzheimer's disease, allowing the alignment of the ~30-year age difference between the cohorts on a clinically meaningful anchor point, namely the participant age at symptomatic onset.

Biomarker profiles were similar for both autosomal dominant Alzheimer's disease and late onset Alzheimer's disease. Both groups demonstrated accelerated rates of decline in cognitive performance and in regional brain volume loss after symptomatic onset. Although amyloid burden accumulation as determined by PET was greater after symptomatic onset in autosomal dominant Alzheimer's disease than in late onset Alzheimer's disease participants, CSF assays of amyloid-β_{42}, amyloid-β_{40}, tau and p-tau$_{181}$ were largely overlapping in both groups. Rates of change in cognitive performance and hippocampal volume loss after symptomatic onset were more aggressive for autosomal dominant Alzheimer's disease participants.

These findings suggest a similar pathophysiology of autosomal dominant Alzheimer's disease and late onset Alzheimer's disease, supporting a shared pathobiological construct.

Received November 29, 2021. Revised April 12, 2022. Accepted April 27, 2022. Advance access publication May 17, 2022

1 Department of Neurology, Washington University School of Medicine, St. Louis, MO, USA
2 Department of Radiology, University of California at San Francisco, San Francisco, CA, USA
3 Division of Biostatistics, Washington University School of Medicine, St. Louis, MO, USA
4 Department of Public Health Sciences, School of Medicine, University of California; Davis, Davis, CA, USA
5 Department of Neurology, Keck School of Medicine, University of Southern California, Los Angeles, CA, USA
6 Department of Cognitive Neurology, Neuropsychology and Neuropsychiatry, Institute for Neurological Research (FLENI), Buenos Aires, Argentina
7 Department of Radiology, Washington University School of Medicine, St. Louis, MO, USA
8 Department of Neurology and Clinical and Translational Science, University of Pittsburgh, Pittsburgh, PA, USA
9 College of Medicine and Health and the Living Systems Institute, University of Exeter, Exeter, UK
10 Alzheimer's Association, Chicago, IL, USA
11 Department of Neurology, Massachusetts General Hospital, Boston, MA, USA
12 Department of Psychiatry, Washington University School of Medicine, St. Louis, MO, USA
13 Department of Neurology, Indiana University School of Medicine, Indianapolis, IN, USA
14 Department of Neurodegenerative Disease and UK Dementia Research Institute, UCL Institute of Neurology, London, UK
15 Department of Pathology and Laboratory Medicine, Indiana University School of Medicine, Indianapolis, IN, USA
16 Ronald M. Loeb Center for Alzheimer's Disease, Department of Genetics and Genomic Sciences, Icahn School of Medicine at Mount Sinai, New York, NY, USA
17 Department of Neurology, Mayo Clinic, Jacksonville, FL, USA
18 Department of Molecular Genetics, Brain Research Institute, Niigata University, Niigata, Japan
19 Department of Radiology, Mayo Clinic, Rochester, MN, USA
20 Helen Wills Neuroscience Institute, University of California, Berkeley, CA, USA
21 Cell Biology of Neurological Diseases Group, German Center for Neurodegenerative Diseases (DZNE), Tübingen, Germany
22 Hertie Institute for Clinical Brain Research, University of Tübingen, Tübingen, Germany
23 DZNE Munich, Munich Cluster of Systems Neurology (SyNergy) and Ludwig-Maximilians-Universität, Munich, Germany
24 Florey Institute, University of Melbourne, Melbourne, Australia
25 Sir James McCusker Alzheimer's Disease Research Unit, Edith Cowan University, Nedlands, Australia
26 Department of Neuroscience, Osaka City University Medical School, Osaka City, Japan
27 Department of Neurology, Taub Institute for Research on Aging Brain, Columbia University Irving Medical Center, New York, NY, USA
28 Department of Neurology, Mayo Clinic, Rochester, MN, USA
29 Department of Neurology, Butler Hospital and Alpert Medical School of Brown University, Providence, RI, 02906, USA
30 Department of Radiology and Imaging Sciences and the Indiana Alzheimer's Disease Research Center, Indiana University School of Medicine, Indianapolis, IN, USA
31 Neuroscience Research Australia and School of Medical Sciences, University of New South Wales, Sydney, Australia
32 Department of Pathology and Laboratory Medicine, Perelman School of Medicine, University of Pennsylvania, Philadelphia, PA, USA
33 Laboratory of Neuro Imaging, Mark and Mary Stevens Neuroimaging and Informatics Institute, Keck School of Medicine, University of Southern California, Los Angeles, CA, USA
34 Center for Neurodegenerative Disease Research, Institute on Aging, Perelman School of Medicine, University of Pennsylvania, Philadelphia, PA, USA
35 German Center for Neurodegenerative Diseases (DZNE) and Department of Neurology, Ludwig-Maximilians-Universität München, Munich, Germany
36 FBRI, Cambridge, MA, USA

Correspondence to: Dr John C. Morris
Knight Alzheimer Disease Research Center
Department of Neurology, 4488 Forest Park Ave
Suite 200, St. Louis, MO 63108, USA
E-mail: jcmorris@wustl.edu

Keywords: Alzheimer pathophysiology; biomarkers; rates of change

Abbreviations: ADAD = autosomal dominant Alzheimer's disease; Aβ = amyloid-beta protein; CDR-SB = Clinical Dementia Rating Sum of Boxes.; DIAN = Dominantly Inherited Alzheimer Network; LOAD = late onset Alzheimer's disease; MC = mutation carrier; PiB = PET radioligand [^{11}C] Pittsburgh Compound B

Introduction

Much knowledge about Alzheimer's disease derives from the study of very rare forms of the disorder that are caused by dominantly inherited pathogenic variants in the *APP*, *PSEN1* and *PSEN2* genes. Indeed, Alzheimer's eponymous case may have been caused by a *PSEN1* pathogenic variant,[1] although the mutation has not been confirmed by DNA sequencing analysis.[2] Transgenic mouse models incorporating *APP* and *PSEN1* mutations have helped elucidate the pathophysiology of Alzheimer's disease[3] and have been critical to the development of mechanism-based investigational drugs for the disease, including immunotherapies that target the amyloid-beta protein (Aβ).[4] Current secondary prevention trials of anti-amyloid experimental therapies in asymptomatic older adults at elevated risk for developing symptomatic Alzheimer's disease[5] first were pioneered in people with autosomal dominant Alzheimer's disease (ADAD).[6–8] However, the extent to which knowledge derived from the study of ADAD pathophysiology extrapolates to the far more common 'sporadic' late onset Alzheimer's disease (LOAD) is uncertain.

There are obvious differences between ADAD and LOAD. Both ADAD and LOAD are characterized by age- and amyloid plaque-dependent reduction in Aβ clearance from the CNS,[9] but only ADAD demonstrates a relative over-production of $A\beta_{42}$ compared with $A\beta_{40}$ and other isoforms.[10] The mean age at symptomatic onset in ADAD is ∼46 years,[11,12] but 95% of symptomatic LOAD persons are age 70 years and older,[13] and correspondingly LOAD very often is complicated by age-associated comorbidities that contribute to the dementia syndrome.[14] The mean age of death in LOAD generally is 82 years or older versus a mean age at death in ADAD of ∼52 years.[15] Thus, both at symptomatic onset and at death, ADAD individuals are approximately three decades younger than LOAD individuals.

Despite these differences, the clinical and neuropathological phenotypes of ADAD and LOAD often are remarkably similar.[11,15,16] Indeed, some ADAD kindreds are clinically indistinguishable from LOAD.[17] The symptomatic onset for both disorders typically is marked by amnestic deficits followed by global cognitive dysfunction and increasing functional impairment. Neuropathological lesion distribution follows an identical hierarchical pattern in both disorders that suggests a common pathophysiological process[18] and immune-electron microscopy shows no difference in tau filament structures in the two disorders.[19] To date, however, a multimodal molecular biomarker comparison of ADAD and LOAD to examine *in vivo* pathophysiology has not been reported. Molecular biomarkers of Alzheimer's disease include cerebral Aβ accumulation as assessed with PET, using radioligands for amyloid, and by altered concentrations of the CSF proteins $A\beta_{42}$, $A\beta_{40}$, tau and p-tau_{181}. A comparative study of these biomarkers is needed to address whether the development and progression of Alzheimer's disease pathophysiology is similar in ADAD and LOAD. A shared pathobiological construct would support the rationale that mechanism-based therapies that demonstrate benefit in ADAD also are likely to be efficacious in LOAD.

Since 2008, the DIAN has established an international multicenter cohort of individuals, both mutation carriers (MCs) and mutation noncarriers, from ADAD families. The Alzheimer's disease neuroimaging intitiative (ADNI) cohort is an ideal LOAD comparator because, like the Dominantly Inherited Alzheimer Network (DIAN), it is a multicenter, longitudinal, international study of multimodal biomarkers of Alzheimer's disease but in non-ADAD older adults. The DIAN and ADNI cohorts both include cognitively normal as well as symptomatic participants. The purpose of the current study was to examine the hypothesis that ADAD and LOAD share similar longitudinal neuroimaging and CSF biomarker profiles, where imaging and CSF data were reprocessed as appropriate to assure uniform pipelines and assays. The focus was on Alzheimer's disease biomarker rates of change in the preclinical stage (prior to symptom onset) and the early symptomatic stage because these stages are the target of secondary prevention[5,20,21] (preclinical Alzheimer's disease) and treatment[22,23] (early symptomatic Alzheimer's disease) trials of investigational anti-Alzheimer therapies. Because phenotypic heterogeneity in ADAD may reflect mutation-specific factors,[16] exploratory analyses were conducted to assess possible effects of pathogenic variants in different genes or in specific codon positions within *PSEN1* on the biomarker characteristics in ADAD.

Materials and methods

All DIAN and ADNI participants self-reported gender, race and ethnicity.

DIAN participants

DIAN recruits and longitudinally assesses biological adult children (age >18 years) of parents with known pathogenic variants causing Alzheimer's disease.[24] From January 2009 to June 2017, DIAN had enrolled 504 participants from 201 ADAD families; three participants had missing pathogenic variant information and were excluded. An additional 21 individuals with the *APP E693Q* (Dutch) pathogenic variant were excluded from the remaining 501 participants because this variant does not result in dementia or neuropathology typical of Alzheimer's disease.[25] Of the remaining 480 participants, 292 were MCs including 224 (76.7%) with a *PSEN1* pathogenic variant (with 71 distinct mutations represented in 131 families), 46 (15.8%) with an *APP* pathogenic variant (with 13 distinct mutations represented in 27 families) and 22 (7.6%) with a *PSEN2* pathogenic variant (with four distinct mutations represented in seven families). The 292 MCs who completed at least their baseline clinical assessment comprised the DIAN cohort in this study.

The DIAN study was approved by each performance site's Institutional Review Board/Ethics Committee, and all participants provided written informed consent. The clinical and cognitive assessments use the Uniform Dataset.[26,27] The information provided by the clinical assessment is synthesized by the clinician to generate the Clinical Dementia Rating® (CDR®),[28] which determines the presence or absence of dementia and, when present, its severity as follows: CDR 0 indicates cognitive normality, whereas CDR 0.5, 1, 2 and 3 indicate very mild, mild, moderate and severe dementia. The CDR yields the more quantitative CDR-Sum Box (CDR-SB) with a range of 0 (no impairment) to 18 (severe impairment).[29] The baseline cognitive assessment includes the Uniform Dataset measures (Table 1). The clinical and the cognitive assessments were conducted independently.

Following the clinical and cognitive assessments, participants had the following procedures: lumbar puncture to obtain CSF, brain MRI and PET with the amyloid radioligand Pittsburgh Compound B (PiB). For asymptomatic participants (i.e. CDR 0), the assessment protocol was obtained approximately every 3 years whereas symptomatic individuals (i.e. CDR > 0) were assessed annually (imaging studies to obtain CSF were completed in participants every 3 years). Of the 292 MCs, 172 participants had two or more visits. Individual research results are not disclosed to the individual.

ADNI participants

Participants were enrolled in ADNI in three waves (ADNI-1, ADNI-GO and ADNI-2) if they were age 55–90 years, had completed

Table 1 Tests and variables used in analyses

Domain	Test/measure
Clinical	
	CDR-SB
	Baseline depression and history of hypertension and diabetes (Type 1 and Type 2)
Cognitive[a]	
	Animal Fluency
	Boston Naming (30 odd items)
	Wechsler Adult Information Scale-Revised Digits Forward
	Wechsler Adult Information Scale-Revised Digits Backward
	Wechsler Memory Scale-Revised-R Logical Memory – Immediate
	Wechsler Memory Scale-Revised Logical Memory – Delayed
	Mini-Mental State Examination
	Trailmaking A
	Trailmaking B
	Wechsler Adult Information Scale-Revised Digit Symbol
	Global composite (all cognitive tests above)
CSF	
	$A\beta_{42}/_{40}$
	tau
	p-tau_{181}
Imaging	
	MRI hippocampal volume
	MRI precuneus thickness
	PET amyloid burden (PIB and florbetapir) expressed in CL

[a]Primary references for each cognitive measure are cited in Weintraub.[27]

at least 6 years of education, were fluent in English and/or Spanish, and met criteria for cognitive normality, mild cognitive impairment or Alzheimer's disease dementia. Recruitment methods at participating ADNI sites included referrals from memory clinics and community outreach programs; all participants provided written informed consent and each performance site's Institutional Review Board approved the ADNI protocol. Clinical and cognitive assessments and brain MRI were completed at baseline and annually thereafter; amyloid PET and CSF were obtained at baseline and every two years thereafter. Details regarding the ADNI protocol, including CDR determination in all participants, and full inclusion and exclusion criteria have been reported[30,31] and are updated at http://adni-info.org. If demented, only ADNI participants with a clinical diagnosis of Alzheimer's disease were included. An amyloid PET scan also was required. Of the 559 ADNI participants who met all criteria, 531 participants had two or more visits.

Comorbid disorders

In both the DIAN and ADNI cohorts, the 15-item Geriatric Depression Scale[32] was administered to all participants at the baseline assessment; a score of five or greater was considered to represent depression. Also at the baseline assessment, participants reported (or, if cognitively impaired, their study partners reported) whether they had been diagnosed with hypertension or diabetes mellitus (Type 1 or Type 2), as these illnesses have acceptable reporting accuracies.[33]

Definition of symptomatic onset

To date, all 45 DIAN MCs with a clinical diagnosis of Alzheimer's disease dementia who were examined neuropathologically had advanced histopathological Alzheimer's disease (Personal communication, Richard J. Perrin, MD, PhD, Washington University). It thus is reasonable to expect that the first recognition of cognitive impairment, as denoted by the assignment of CDR > 0 during a clinical assessment, in an MC represents the initial symptomatic manifestation of Alzheimer's disease. The time of symptomatic onset for DIAN MCs was defined as the time of the first score of CDR > 0 or on the estimated age at symptomatic onset as determined by genetic and parental data.[12] Neuropathological confirmation of Alzheimer's disease in ADNI participants with a clinical diagnosis of mild cognitive impairment or of Alzheimer's disease dementia, however, is less certain. For example, in one study of 526 participants assessed at National Institute on Aging-funded Alzheimer Disease Centers, 88 (16.7%) individuals with a diagnosis of clinically probable Alzheimer's disease did not meet neuropathologic criteria for the disease.[34] At the earliest stages of cognitive impairment, it can be difficult to distinguish Alzheimer's disease as the underlying aetiology from other potential non-progressive causes of cognitive dysfunction such as depression and polypharmacy.[35] ADNI participants thus were required to demonstrate progressive cognitive dysfunction as operationalized by an increase of the individual's CDR-SB of 1 or greater, and symptomatic onset for ADNI participants was the time when progression of CDR-SB ≥ 1 occurred.

Cognitive data

Ten cognitive tests (Table 1) were shared between DIAN and ADNI cognitive batteries: Animal Fluency, Boston Naming, Wechsler Adult Intelligence Scale-Revised Digits Forward and Backward, Wechsler Memory Scale-Revised Logical Memory-Immediate and Delayed Recall, Mini Mental State Examination (MMSE), Trailmaking A, Trailmaking B and Wechsler Adult Intelligence Scale-Revised Digit Symbol.[27] For each test, a Z-score was computed by using the mean and standard deviation (SD) of all the data from the combined cohort. A cognitive composite was derived by averaging the 10 Z-scores (with appropriate re-orientation of the tests so that higher values of all tests in the composite were associated with better cognitive performance).

Genetics

For the DIAN participants, sequence analysis for specific pathogenic variants and *APOE* genotyping were performed as previously described.[36] ADNI participant *APOE* ϵ2, ϵ3 and ϵ4 isoforms were determined in accordance with published methods.[37]

CSF

Collection of CSF in both DIAN and ADNI was in accordance with standard protocols. Briefly, ~15–25 ml of CSF was collected in polypropylene tubes at 8:00 am following overnight fasting and immediately frozen on dry ice. Frozen samples were shipped overnight on dry ice to the respective Biomarker Cores for DIAN and ADNI, where after thawing they were aliquoted (0.5 ml), flash-frozen on dry ice and stored at −80°C until the day of analysis. For this study, aliquots from stored samples of DIAN participants were shipped on dry ice to the ADNI Biomarker Core for biomarker analysis. The Roche Elecsys immunoassays for $A\beta_{42}$, $A\beta_{40}$, tau and p-tau_{181} measurements in CSF were performed on a Cobas e601 instrument as previously described.[38–40] A single lot number of reagents for each of the four analytes was used throughout this study. Note that the ratio of CSF $A\beta_{42}$ to $A\beta_{40}$ is considered to be superior to the CSF concentration of $A\beta_{42}$ alone in detecting Alzheimer's disease pathology,[39] and thus only the ratio is considered in this study.

The 424 ADNI (obtained from 181 participants) and 627 DIAN (obtained from 235 participants) CSF samples were run in singlicate for each of the four biomarker analytes. The samples were randomly distributed across runs on 14 days and were completed over the time period of 18 October 2017 through 9 November 2017.

Quality control results were within stated limits to meet acceptance criteria for precision and accuracy and ~40 samples were run twice each day for 14 days. Lower and upper technical limits for each Elecsys analyte measuring range were 200–1700 pg/ml for CSF $A\beta_{42}$, 22–40 300 pg/mL for CSF $A\beta_{40}$, 80–1300 pg/ml for CSF tau and 8–120 pg/ml for CSF p-tau_{181}. All other methodologic details are as described.[40]

Imaging

MRI imaging for both projects was based on the ADNI protocols. Due to budgetary limitations, only ADNI participants with two or more amyloid PET scans had their scans reprocessed. All raw ADNI MRI and PET data were downloaded from http://adni.loni.usc.edu/ by the DIAN Imaging Core for reprocessing to ensure harmonization between the two cohorts. DIAN T_1-weighted sequences were acquired on a 3 T scanner with a 1.1 × 1.1 × 1.2 mm resolution. ADNI data were acquired on a mixture of 1.5 T ($n = 260$) and 3 T ($n = 535$) scans[41] with resolutions of <1.3 mm (http://adni.loni.usc.edu/methods/documents/mri-protocols).

A total of 514 DIAN and 865 ADNI T_1-weighted structural MRI scans underwent volumetric segmentation and cortical surface reconstruction using FreeSurfer v.5.3.[42,43] For all statistical analyses, the cortical thickness was averaged and volume measures were summed across hemispheres. Regional volumes were corrected for intracranial volume using a regression approach.[44] On the basis of studies of regions sensitive to volume loss in ADAD and LOAD, the LOAD cortical signature emphasized atrophy in temporal lobe regions whereas the ADAD signature was focused on parietal regions.[45] Hence, hippocampal volumes and precuneus thickness were selected for analysis. Details of processing and quality control criteria were described previously.[46,47] A total of 512 DIAN and 798 ADNI FreeSurfer MRI process passed the quality control procedures.

For amyloid PET scans, two radioligands, PiB and florabetapir, were used in accordance with standard protocols.[48,49] A total of 512 PiB scans from the DIAN cohort and 802 (679 florbetapir and 123 PiB) scans from the ADNI cohort were processed. Quality control criteria for PET processes pipeline included post-injection window of 40–70 min for PiB and 50–70 min for florbetapir; and the availability of MRI scan within 24 months of the PET scan with passed FreeSurfer process. Thus, the total number included in this analysis are 429 PiB scans from the DIAN cohort and 586 (535 florbetapir and 51 PiB) scans from the ADNI cohort.

Amyloid deposition in the regions of interest was determined using FreeSurfer, and a standardized uptake value ratio with correction for partial volume effects was calculated (https://github.com/ysu001/PUP).[46,47] The cerebellum was chosen as the reference region. PET scans were smoothed with an 8 mm Gaussian kernel to achieve a common spatial resolution across scanners. All data were partial volume corrected using a geometric transfer matrix approach.[50,51] A composite measure to represent a global measure of Aβ was calculated using the averaged standardized uptake value ratios in the lateral orbitofrontal, medial orbitofrontal, precuneus, rostral middle frontal, superior frontal, superior temporal and middle temporal regions. Values from this global summary were converted to the Centiloid (CL) scale[52] to harmonize tracer and data processing differences using our previously published equations.[47,53]

Statistical analysis

The variables used for analysis are shown in Table 1. Baseline characteristics of the DIAN MCs and ADNI participants were summarized separately with proportions for categorical variables and means and SD for quantitative variables. Because ADNI and DIAN used different tracers in amyloid PET imaging, the mean cortical standardized uptake value ratios from both databases were converted to the CL scale for analyses.[52,53]

For the primary comparisons of longitudinal change on biomarkers and cognitive outcomes, the longitudinal courses were aligned by a clinically meaningful anchor (i.e. age at symptom onset). The anchor point for DIAN participants who had yet to reach a global CDR of 0.5 or higher during longitudinal follow-up was their mutation-based age at symptom onset (or their parental age of symptom onset if the former was not available).[12] For each DIAN participant whose global CDR had progressed from 0 at baseline to at least 0.5 during longitudinal follow-up, his/her age at the visit when a CDR 0.5 or above was first rendered served as the anchor point. For ADNI participants with a CDR-SB <1 at baseline, the anchor point was the age when a CDR-SB of 1 or higher first was observed, either at baseline or during longitudinal follow-up. The anchor point for ADNI participants whose baseline CDR-SB already was larger than 1 was estimated through a calibration after fitting a random intercept model[54] to the observed CDR-SB in this group.

For each participant from DIAN and ADNI, the estimated years to symptomatic onset[12] was defined as the difference between the participant's age at each visit and the age of the anchor point. Hence, an estimated years to onset of 0 indicates the anchor point, and negative and positive estimated years to onset indicate the asymptomatic and symptomatic stages, respectively. After aligning all longitudinal data at the anchor point across participants for each biomarker and cognitive outcome, we used estimated years to onset as the time scale and fitted mixed-effects piecewise linear models with a random intercept and two random slopes.[54] The models assumed, for each cohort, a piecewise linear trend preceding and following the anchor point as the primary fixed effects of interest. This approach allowed the longitudinal trajectories to be assessed for differences between DIAN MCs and ADNI participants, both before and after the clinical anchor point, by estimating and testing the difference of the corresponding slopes between the two cohorts in the model. Further analyses included *APOE* ε4 status, gender and education as the additional fixed effects, and these effects were examined on the comparisons between DIAN MCs and ADNI participants. Additionally, all two-way interactive effects between cohorts, gender, education and *APOE* ε4 status were examined on the rates of longitudinal change. Exploratory analyses as to whether the effects of mutations in different genes or in specific codon positions within *PSEN1* affected biomarker change in the DIAN MCs were conducted. The residuals were examined for evidence of non-normality, non-linearity and other potential model violations. These models led to approximate two-sided *t*-tests for comparing the slopes between the two cohorts, with the degrees of freedom estimated by the Satterthwaite method. Statistical significance was defined as $P < 0.05$. All analyses were carried out in SAS v.9.4.[55] All data are reported in the text, tables and or figures (CSF $A\beta_{42}$ and CSF $A\beta_{40}$ are reported as the ratio, CSF $A\beta_{42/40}$).

Data and materials availability

All data and code use in these analyses are available to any researcher for purposes of reproducing or extending the analyses. To protect the

privacy of research participants, investigators must sign a data use agreement with the respective institutions. Data may be requested at the following websites: DIAN at https://dian.wustl.edu/our-research/for-investigators/dian-observational-study-investigator-resources/ and ADNI data: http://adni.loni.usc.edu/. There was no blinding or randomization in this study.

Results

The variables available for analysis are shown in Table 1 and are discussed in the 'Materials and methods' section. The baseline demographic features for the DIAN and ADNI cohorts, each in two groups based on CDR score (i.e. CDR 0 versus CDR > 0) are shown in Table 2. Asymptomatic ADNI participants (i.e. CDR 0) were ∼40 years older than their DIAN counterparts; symptomatic ADNI participants (i.e. CDR > 0) were ∼30 years older than symptomatic DIAN individuals. Both asymptomatic and symptomatic ADNI participants had more years of education than corresponding DIAN participants. For the symptomatic groups, ADNI participants were more likely to be male and to carry an $\epsilon 4$ allele of the *APOE* gene compared with symptomatic DIAN MCs. At baseline, symptomatic DIAN participants were more cognitively impaired than their ADNI counterparts as measured by MMSE scores. Limited information about baseline comorbid disorders was available (not shown in Table 1). Fifty-seven (19.5%) DIAN MCs were depressed, 22 (7.5%) reported a history of hypertension and four (1.4%) reported a history of diabetes mellitus. Twenty-nine (5%) of ADNI participants were depressed, 265 (47.4%) reported a history of hypertension and 59 (10.6%) reported a history of diabetes mellitus.

As noted in Figs 1 and 2, the transition from asymptomatic to symptomatic for both the DIAN and ADNI groups was marked by an inflection at the anchor point in rates of change for CDR-SB, cognitive composite, and brain MRI-derived loss of hippocampal volume and precuneus cortical thickness such that the rates increased after symptomatic onset. To examine rates of change before and after age at symptomatic onset, results are shown as within cohort comparisons as well as comparisons between cohorts. Note that most DIAN participants do not know, nor do they wish to learn, their mutation status. To reduce the possibility of unintended disclosure that a DIAN individual may be a mutation carrier, data points from the 48 participants who were >20 years younger than their estimated age at symptomatic onset are not displayed in Figs 1–4, although all data were used in the analyses.

Clinical Dementia Rating Sum of Boxes and cognitive composite

Within cohorts

DIAN MCs had a greater rate of increase on the CDR-SB ($P < 0.0001$, $t = -19.36$) and a greater rate of decline on the cognitive composite ($P < 0.0001$, $t = 14.92$) after symptomatic onset compared with the rates of change prior to symptomatic onset. Similarly, the rates of change on the CDR-SB and the cognitive composite in ADNI participants was greater after symptomatic onset compared with the rates of change prior to symptomatic onset ($P < 0.0001$, $t = -16.13$ and $P < 0.0001$, $t = 16.60$, respectively). See Fig. 1 and Table 3.

Between cohorts

ADNI participants had a greater increase in CDR-SB scores prior to symptomatic onset in comparison with DIAN MCs ($P < 0.001$, $t = 4.75$). The rates of decline on the cognitive composite did not differ for DIAN MCs and ADNI participants before symptomatic onset. However, after symptomatic onset the DIAN MCs had greater rates of change than did the ADNI participants on the CDR-SB ($P < 0.001$, $t = -7.11$) and the cognitive composite ($P < 0.0001$, $t = 6.92$). See Fig. 1 and Table 4.

Cerebral volume loss

Within cohorts

Hippocampal volume loss occurred prior to symptomatic onset for both DIAN MCs and ADNI participants ($P \leq 0.0007$, $t = -3.45$ and $P < 0.0001$, $t = -6.58$, respectively). The rates of loss of hippocampal volume and of precuneus thickness were increased after symptomatic onset when compared with rates before symptomatic onset for both DIAN MCs ($P < 0.0001$, $t = 12.34$ for hippocampal volume and $P < 0.0001$, $t = 11.59$ for precuneus thickness) and for ADNI participants ($P < 0.0001$, $t = 4.97$ for hippocampal volume and $P = 0.0005$, $t = 3.47$ for precuneus thickness). See Fig. 2 and Table 3.

Table 2 Group characteristics at baseline

	ADNI participants $n = 559$		DIAN mutation carriers $n = 292$			
	CDR = 0 $n = 72$ (13%)	CDR > 0 $n = 487$ (87%)	CDR = 0 $n = 185$ (63%)	CDR > 0 $n = 107$ (37%)	DIAN versus ADNI CDR = 0 *P*-value	DIAN versus ADNI CDR > 0 *P*-value
Age, years, mean (SD)	75.2 (5.6)	73.6 (7.6)	33.5 (8.8)	46.0 (10.0)	<0.0001	<0.0001
Gender (% Female)	51.4	39.4	57.3	51.4	0.3890	0.0233
Race (% Non-Hispanic White or White)	93.1	95.5	87.6	92.5	0.2115	0.2108
Education, years, mean (SD)	16.1 (2.8)	15.9 (2.8)	14.8 (2.9)	13.4 (3.1)	0.0006	<0.0001
MMSE, mean (SD)	29.1 (1.0)	26.1 (2.8)	29.1 (1.2)	22.5 (6.9)	0.9730	<0.0001
APOE $\epsilon 4$						
1 $\epsilon 4$ allele	22 (30.6%)	215 (44.2%)	52 (28.1%)	28 (26.2%)	0.7124	0.0004
2 $\epsilon 4$ alleles	1 (1.4%)	75 (15.4%)	2 (1.1%)	6 (5.6%)	0.9395	0.0017
Clinical f/u, years, mean (SD)	5.8 (3.2)	3.5 (2.5)	3.4 (1.5)	2.5 (1.5)	<0.0001	0.0011

f/u = follow-up.

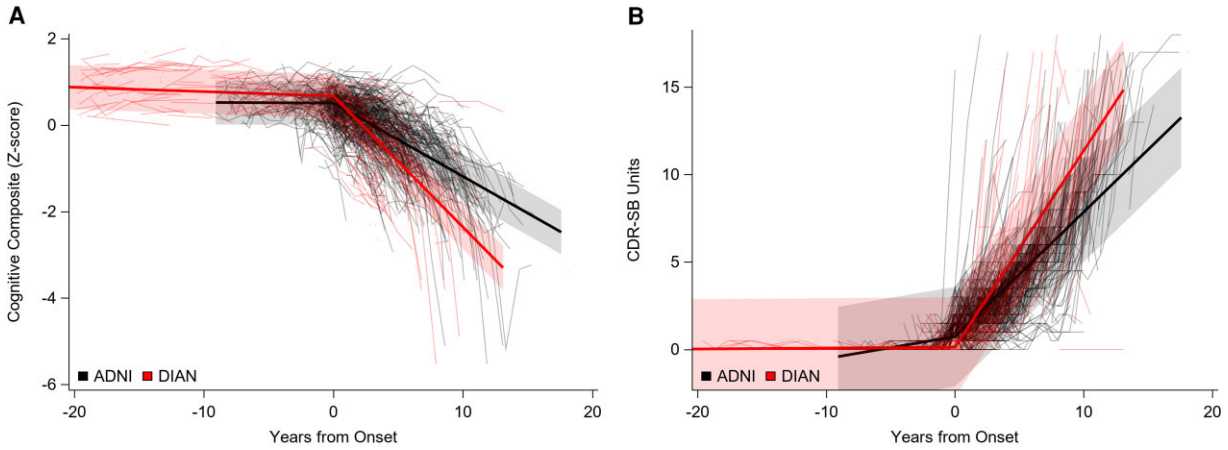

Figure 1 Individual performance (spaghetti plots) and group mean rates of change (solid lines) over time for cognitive composite and clinical evaluation. (**A**) The cognitive composite and (**B**) the CDR-SB. Data from DIAN participants are displayed in red and data from ADNI participants are shown in black. In all parts, 0 represents the time of symptom onset.

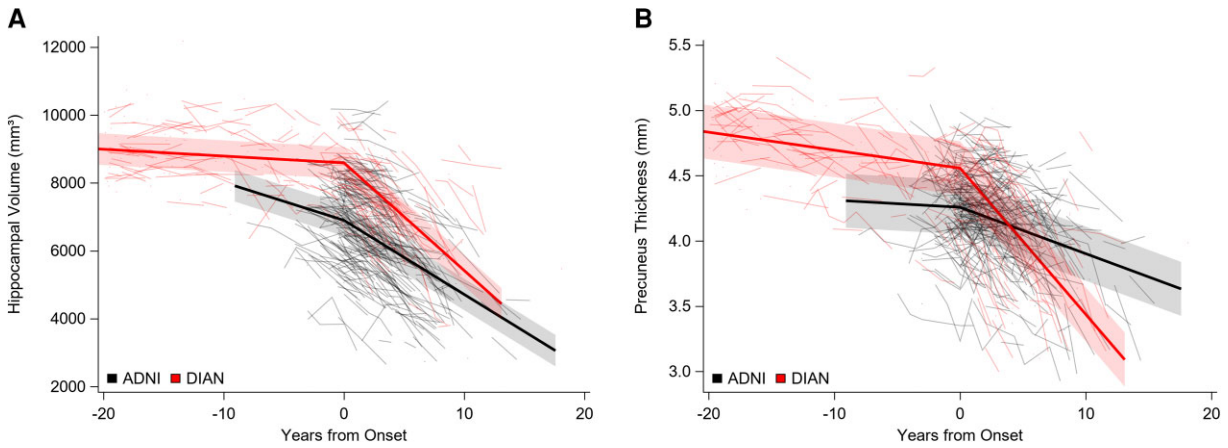

Figure 2 Individual performance (spaghetti plots) and group mean rates of change (solid lines) over time for hippocampal volume and precuneus thickness. (**A**) Hippocampal volume in mm^3 and (**B**) precuneus thickness in mm. In all parts, 0 represents the time of symptom onset.

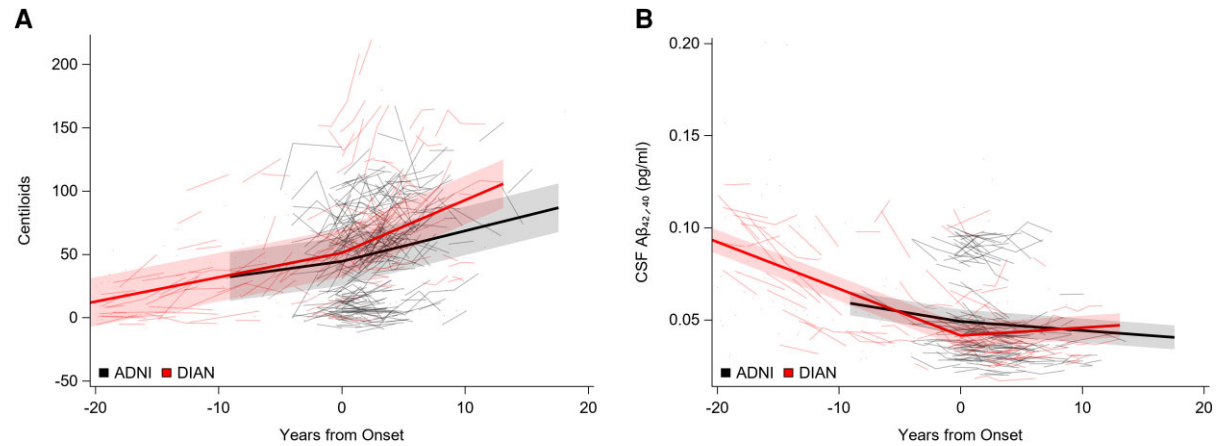

Figure 3 Individual performance (spaghetti plots) and group mean rates of change (solid lines) over time for amyloid imaging and CSF amyloid ratio. (**A**) Cerebral amyloid accumulation in CL and (**B**) the CSF $A\beta_{42/40}$ ratio in pg/ml. In all parts, 0 represents the time of symptom onset.

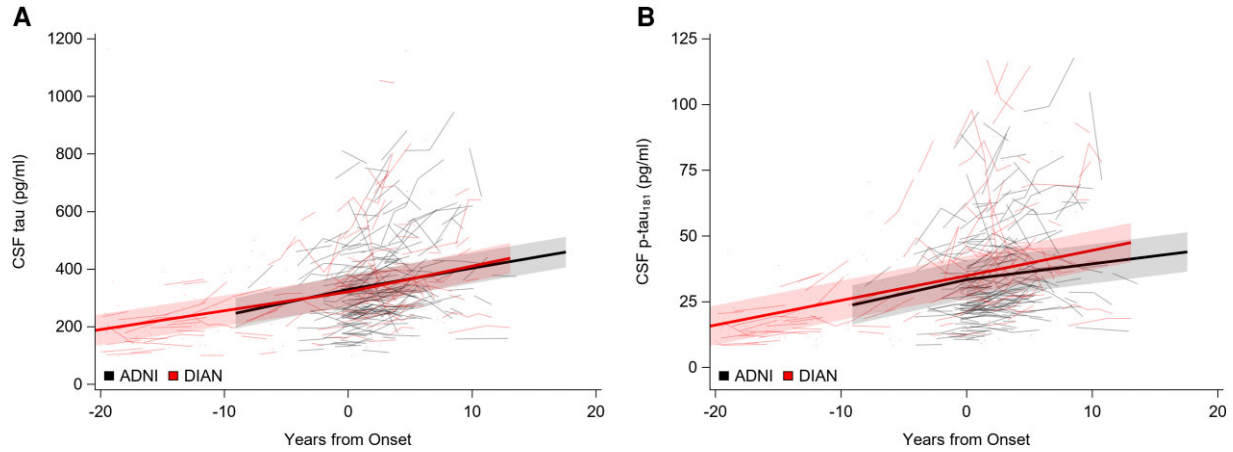

Figure 4 Individual performance (spaghetti plots) and group mean rates of change (solid lines) over time for CSF tau. (**A**) Concentrations of CSF tau in pg/ml and (**B**) p-tau$_{181}$ in pg/ml. In all parts, 0 represents the time of symptom onset.

Between cohorts

Consistent with the recognized decline in brain volume with age,[56,57] ADNI participants had a greater rate of decline in hippocampal volume prior to symptomatic onset than did DIAN MCs ($P < 0.001$, $t = 5.11$); there was no cohort difference in loss of precuneus thickness prior to symptomatic onset. After symptomatic onset, DIAN MCs when compared with ADNI participants had a greater rate of loss in both hippocampal volume ($P < 0.001$, $t = 4.02$) and precuneus thickness ($P < 0.001$, $t = 8.75$). See Fig. 2 and Table 4.

Amyloid status

Within cohorts

DIAN MCs started accumulating amyloid prior to symptomatic onset ($P < 0.0001$, $t = 14.42$), and had an increased rate of cerebral amyloid accumulation on the CL scale after symptomatic onset when compared with the rate before symptomatic onset ($P = 0.0024$, $t = 3.07$). The rate of cerebral amyloid accumulation did not differ for ADNI participants before or after symptomatic onset. A decrease in the ratio of CSF Aβ_{42} to Aβ_{40} (A$\beta_{42/40}$) occurred prior to symptomatic onset for both ADNI participants ($P = 0.017$, $t = 2.41$) and DIAN MCs participants ($P < 0.001$, $t = 12.69$). Perhaps as a consequence of an initial elevated threshold due to the marked over-production of Aβ_{42} in MCs, the rate of decline in CSF A$\beta_{42/40}$ levels for DIAN MCs was greater before symptomatic onset than afterward ($P < 0.0001$, $t = 8.55$). In ADNI participants, the rate of decline in CSF A$\beta_{42/40}$ did not differ before or after symptomatic onset. See Fig. 3 and Table 3.

Between cohorts

There was no difference between DIAN MCs and ADNI participants in the rate of cerebral amyloid accumulation measured by CL before symptomatic onset. After symptomatic onset, DIAN MCs had a greater rate of cerebral amyloid accumulation than did ADNI participants ($P = 0.0221$, $t = 2.31$). DIAN MCs had a greater rate of decline in CSF A$\beta_{42/40}$ than ADNI participants before symptomatic onset ($P = 0.0034$, $t = 2.96$), possibly because of the notably increased baseline CSF Aβ_{42} levels that characterizes ADAD, but after symptomatic onset ADNI participants had a greater rate of decline ($P = 0.0022$, $t = 3.14$). See Fig. 3 and Table 4.

CSF tau and p-tau$_{181}$

Within cohorts

The rates of increase in CSF concentrations of tau and p-tau$_{181}$ did not differ for DIAN MCs and ADNI participants whether before or after symptomatic onset for either the DIAN MCs or the ADNI participants. See Fig. 4 and Table 3.

Between cohorts

The rates of change in CSF concentrations of tau and p-tau181 did not differ for DIAN MCs when compared with ADNI participants, either before or after symptomatic onset. See Fig. 4 and Table 4.

Adjustment for covariates

All between cohort findings remained as reported in Table 4 after adjustment for gender, years of education and *APOE* ϵ4 status (Supplementary Table 1), and additionally for presence of depression, hypertension and diabetes (Supplementary Table 2).

Adjustment for potential participants without Alzheimer's disease

Sixty-seven ADNI participants had a CSF AB$_{42/40}$ ratio above 0.063 with the Elecsys immunoassay; a ratio below 0.063 is considered indicative of Alzheimer neuropathology (L.M. Shaw, personal communication). Several factors might explain the higher ratio in the 67 ADNI participants (the 67 also included 13 ADNI participants who did not demonstrate increased amyloid PET burden after symptomatic onset), but one possibility is that these individuals had a non-Alzheimer dementing disorder. All analyses were repeated without data from the 67 participants to assess whether their inclusion may have skewed the ADNI cohort results. However, the re-analyses did not change any of the comparisons of the DIAN and ADNI cohorts with the exception that the significantly higher amyloid PET burden for DIAN participants when all 559 ADNI participants were analysed (Table 4) no longer is significant (Supplementary Table 3).

APOE ϵ4 effects

Further analyses examined all two-way interactions between cohorts, gender, years of education, and *APOE* ϵ4 status on the rates

Table 3 Within-group comparisons of rates of change in ADNI participants ($n = 559$) and in DIAN mutation carriers ($n = 292$)

	ADNI slopes			DIAN MC slopes		
	Before onset	After onset	Difference	Before onset	After onset	Difference
CDR-SB	0.125 (0.024) [$P < 0.0001$, $t = 5.29$]	0.713 (0.022) [$P < 0.0001$, $t = 32.00$]	−0.5873 {−0.6587 to −0.5159} [$P < 0.0001$, $t = -16.13$]	0.005 (0.009) [$P = 0.5570$, $t = 0.59$]	1.124 (0.053) [$P < 0.0001$, $t = 21.04$]	−1.1189 {−1.2324 to −1.0055} [$P < 0.0001$, $t = -19.36$]
Cognitive composite	−0.001 (0.006) [$P = 0.8000$, $t = -0.25$]	−0.170 (0.008) [$P < 0.0001$, $t = -21.70$]	0.1685 {0.1485 to 0.1885} [$P < 0.0001$, $t = 16.60$]	−0.010 (0.004) [$P = 0.0060$, $t = -2.78$]	−0.304 (0.018) [$P < 0.0001$, $t = -17.18$]	0.2935 {0.2549 to 0.3321} [$P < 0.0001$, $t = 14.92$]
Hippocampal volume (mm^3)	−111.960 (17.007) [$P < 0.0001$, $t = -6.58$]	−218.370 (11.286) [$P < 0.0001$, $t = -19.35$]	106.41 {64.36 to 148.47} [$P < 0.0001$, $t = 4.97$]	−20.077 (5.820) [$P = 0.0007$, $t = -3.45$]	−317.180 (21.801) [$P < 0.0001$, $t = -14.55$]	297.10 {249.78 to 344.43} [$P < 0.0001$, $t = 12.34$]
Precuneus thickness (mm)	−0.005 (0.007) [$P = 0.4638$, $t = -0.79$]	−0.036 (0.004) [$P < 0.0001$, $t = -8.55$]	0.03010 {0.01308 to 0.04713} [$P = 0.0005$, $t = 3.47$]	−0.014 (0.002) [$P < 0.0001$, $t = -7.46$]	−0.112 (0.008) [$P < 0.0001$, $t = -14.59$]	0.09817 {0.08152 to 0.1148} [$P < 0.0001$, $t = 11.59$]
Amyloid PET (mean CL)	1.343 (0.810) [$P = 0.0980$, $t = 1.66$]	2.406 (0.355) [$P < 0.0001$, $t = 6.77$]	−1.0634 {−2.8856 to 0.7588} [$P = 0.2522$, $t = -1.15$]	1.924 (0.133) [$P < 0.0001$, $t = 14.42$]	4.169 (0.675) [$P < 0.0001$, $t = 6.17$]	−2.2449 {−3.6862 to −0.8036} [$P = 0.0024$, $t = -3.07$]
CSF $A\beta_{42/40}$ (pg/ml for both CSF $A\beta_{42}$ and CSF $A\beta_{40}$)	−0.001 (0.0004) [$P = 0.0170$, $t = -2.41$]	−0.0005 (0.0001) [$P = 0.0016$, $t = -3.24$]	−0.0006 {−0.00158 to 0.000382} [$P = 0.2309$, $t = -1.20$]	−0.003 (0.0002) [$P < 0.0001$, $t = -12.69$]	0.0004 (0.0002) [$P = 0.0899$, $t = 1.71$]	−0.00297 {−0.00366 to −0.00229} [$P < .0001$, $t = -8.55$]
CSF tau (pg/ml)	9.086 (2.701) [$P = 0.0009$, $t = 3.36$]	7.395 (2.000) [$P = 0.0003$, $t = 3.70$]	1.6916 {−5.3726 to 8.7558} [$P = 0.6381$, $t = 0.47$]	6.543 (0.662) [$P < 0.0001$, $t = 9.88$]	8.952 (3.157) [$P = 0.0050$, $t = 2.84$]	−2.4092 {−9.1078 to 4.2894} [$P = 0.4794$, $t = -0.71$]
CSF p-tau_{181} (pg/ml)	1.062 (0.373) [$P = 0.0049$, $t = 2.85$]	0.599 (0.268) [$P = 0.0265$, $t = 2.24$]	0.4630 {−0.5207 to 1.4466} [$P = 0.3554$, $t = 0.9$]	0.937 (0.085) [$P < 0.0001$, $t = 11.00$]	0.966 (0.407) [$P = 0.0184$, $t = 2.38$]	−0.02836 {−0.9053 to 0.8486} [$P = 0.9493$, $t = -0.06$]

Values in parentheses represent the standard error of the estimates. Values in brackets represent the P-value and t-statistic, where degrees of freedom were estimated with the Satterthwaite method for testing whether the group-specific rates of change are equal to 0 with a two-sided t-test. The range in braces is the 95% confidence interval for the difference in slopes before and after symptom onset within cohort. Unadjusted analyses used unstructured covariance matrix among random effects, except CSF $A\beta_{42/40}$ and CDR-SB that used variance components.

of longitudinal change. There were no significant interactions between the cohorts and gender, years of education and *APOE ϵ4* status with any biomarker. For example, the estimated annual rate of increase after symptomatic onset of amyloid accumulation (CL) for DIAN MCs with and without an ϵ4 allele was 0.379 versus 0.357 and for ADNI participants with and without an ϵ4 was 0.217 versus 0.213. A trend was noted for the cognitive composite after symptomatic onset ($P = 0.0572$, $t = 1.91$); although DIAN MCs with and without an ϵ4 allele shared almost the same annual rate of decline (−0.283 versus −0.278 per year), ADNI participants with an ϵ4 allele had a faster rate of decline (−0.210 per year) than ADNI participants without an ϵ4 allele (−0.130 per year).

Gene- and mutation-specific effects in DIAN mutation carriers

No consistent gene- or mutation-specific biomarker effects were noted in the exploratory analyses, which were limited by small sample sizes (46 *APP* and 22 *PSEN2* mutations) and by the multiplicity effects of many comparisons (Supplementary Tables 4 and 5). However, prior to symptom onset, *PSEN1* MCs had a greater loss of hippocampal volume than *APP* MCs. Also before symptom onset, *PSEN1* MCs had a greater increase in CSF p-tau_{181} than *APP* MCs and a greater decrease in CSF $A\beta_{42/40}$ than *PSEN2* MCs.

Discussion

To our knowledge, this study represents the first longitudinal comparison of identically assessed molecular biomarkers of Alzheimer's disease in ADAD and LOAD. The results support the following conclusions: (i) molecular biomarker profiles for cerebral amyloidosis and tauopathy are similar in ADAD and LOAD; (ii) in both ADAD and LOAD, rates of change in cognitive impairment and in loss of hippocampal volume and precuneus thickness accelerate after symptomatic onset; and (iii) after symptomatic onset, ADAD has a more aggressive course than LOAD as measured by rates of cognitive decline and regional brain volume loss and possibly by greater cerebral amyloid accumulation (without the 67 ADNI participants who may have had a non-Alzheimer dementia, cerebral amyloid accumulation after symptomatic onset between DIAN and ADNI participants did not differ significantly). The more rapid cognitive decline after symptomatic onset for ADAD compared to LOAD also was demonstrated in a similar study using a different LOAD cohort than ADNI.[58] There were no significant interactions for any biomarker between the ADAD and LOAD cohorts and *APOE ε4* status. On the basis of limited evidence, there were no consistent gene- or mutation-specific differences to preclude comparison of the combined DIAN cohort with the ADNI cohort. Two putative markers of neurodegeneration, CSF tau levels and cerebral volume loss, had divergent outcomes after symptomatic onset in that the rate of change for CSF tau

Table 4 Between-group comparisons of rates of change between ADNI participants ($n = 559$) and DIAN mutation carriers ($n = 292$)

	Slope before onset			Slope after onset		
	ADNI	DIAN MC	Difference	ADNI	DIAN MC	Difference
CDR-SB	0.125 (0.024) [$P < 0.0001$, $t = 5.29$]	0.005 (0.009) [$P = 0.5570$, $t = 0.59$]	0.1203 {0.07057 to 0.1700} [$P < 0.0001$, $t = 4.75$]	0.713 (0.022) [$P < 0.0001$, $t = 32.00$]	1.124 (0.053) [$P < 0.0001$, $t = 21.04$]	−0.4114 {−0.5250 to −0.2977} [$P < 0.0001$, $t = -7.11$]
Cognitive composite	−0.001 (0.006) [$P = 0.8000$, $t = -0.25$]	−0.010 (0.004) [$P = 0.0060$, $t = -2.78$]	0.008659 {−0.00454 to 0.02185} [$P = 0.1971$, $t = 1.29$]	−0.170 (0.008) [$P < 0.0001$, $t = -21.70$]	−0.304 (0.018) [$P < 0.0001$, $t = -17.18$]	0.1337 {0.09574 to 0.1716} [$P < 0.0001$, $t = 6.92$]
Hippocampal volume (mm^3)	−111.960 (17.007) [$P < 0.0001$, $t = -6.58$]	−20.077 (5.820) [$P = 0.0007$, $t = -3.45$]	−91.8785 {−127.20 to −56.5541} [$P < 0.0001$, $t = -5.11$]	−218.370 (11.286) [$P < 0.0001$, $t = -19.35$]	−317.180 (21.801) [$P < 0.0001$, $t = -14.55$]	98.8084 {50.5416 to 147.08} [$P < 0.0001$, $t = 4.02$]
Precuneus thickness (mm)	−0.005 (0.007) [$P = 0.4638$, $t = -0.79$]	−0.014 (0.002) [$P < 0.0001$, $t = -7.46$]	0.008310 {−0.00582 to 0.02244} [$P = 0.2485$, $t = 1.16$]	−0.036 (0.004) [$P < 0.0001$, $t = -8.55$]	−0.112 (0.008) [$P < 0.0001$, $t = -14.59$]	0.07638 {0.05921 to 0.09355} [$P < 0.0001$, $t = 8.75$]
Amyloid PET (mean CL)	1.343 (0.810) [$P = 0.0980$, $t = 1.66$]	1.924 (0.133) [$P < 0.0001$, $t = 14.42$]	−0.5809 {−2.1937 to 1.0319} [$P = 0.4794$, $t = -0.71$]	2.406 (0.355) [$P < 0.0001$, $t = 6.77$]	4.169 (0.675) [$P < 0.0001$, $t = 6.17$]	−1.7624 {−3.2690 to −0.2558} [$P = 0.0221$, $t = -2.31$]
CSF $A\beta_{42/40}$ (pg/ml for both CSF $A\beta_{42}$ and CSF $A\beta_{40}$)	−0.001 (0.0004) [$P = 0.0170$, $t = -2.41$]	−0.003 (0.0002) [$P < 0.0001$, $t = -12.69$]	0.00146 {0.000487 to 0.002432} [$P = 0.0034$, $t = 2.96$]	−0.0005 (0.0001) [$P = 0.0016$, $t = -3.24$]	0.0004 (0.0002) [$P = 0.0899$, $t = 1.71$]	−0.00091 {−0.00149 to −0.00034} [$P = 0.0022$, $t = -3.14$]
CSF tau (pg/ml)	9.086 (2.701) [$P = 0.0009$, $t = 3.36$]	6.543 (0.662) [$P < 0.0001$, $t = 9.88$]	2.5435 {−2.9352 to 8.0222} [$P = 0.3613$, $t = 0.91$]	7.395 (2.000) [$P = 0.0003$, $t = 3.70$]	8.952 (3.157) [$P = 0.0050$, $t = 2.84$]	−1.5573 {−8.9195 to 5.8049} [$P = 0.6771$, $t = -0.42$]
CSF p-tau_{181} (pg/ml)	1.062 (0.373) [$P = 0.0049$, $t = 2.85$]	0.937 (0.085) [$P < 0.0001$, $t = 11.00$]	0.1251 {−0.6292 to 0.8794} [$P = 0.7442$, $t = 0.33$]	0.599 (0.268) [$P = 0.0265$, $t = 2.24$]	0.966 (0.407) [$P = 0.0184$, $t = 2.38$]	−0.3663 {−1.3260 to 0.5935} [$P = 0.4526$, $t = -0.75$]

Values in parentheses represent the standard error of the estimates. Values in brackets represent the *P*-value and *t*-statistic, where degrees of freedom were estimated with the Satterthwaite method for testing whether the group-specific rates of change are equal to 0 with a two-sided *t*-test. The range in braces is the 95% confidence interval for the difference in slopes between the two cohorts. Unadjusted analyses used unstructured covariance matrix among random effects, except CSF $A\beta_{42/40}$ and CDR-SB that used variance components.

did not differ between ADAD and LOAD, whereas the rates of change for hippocampal volume loss and decreased precuneus thickness were accelerated in ADAD compared with LOAD. This divergence seemingly is inconsistent with a proposed biomarker-based definition of Alzheimer's disease wherein both CSF tau and cortical atrophy are considered to represent non-specific neural injury.[59] However, subsequent to this study, there is emerging consensus that CSF levels of neurofilament light may be a better indicator than CSF tau of neurodegeneration in Alzheimer's disease.[60]

Prevention trials in LOAD are limited by the uncertainty of whether all cognitively normal individuals with preclinical Alzheimer's disease will inevitably transition to symptomatic Alzheimer's disease and, if they do, when the transition will occur. Moreover, studies of LOAD may be confounded by the effects of age and comorbidities. In contrast, asymptomatic ADAD MCs are virtually certain to develop symptomatic Alzheimer's disease (the pathogenic variants have near 100% penetrance) and at a predictable age;[12] they typically also are free of most age-associated co-pathologies.[15] Thus, secondary prevention trials in ADAD MCs may be a valuable paradigm for analogous trials in LOAD. This study demonstrates that molecular biomarkers for Alzheimer's disease have similar profiles in ADAD and in LOAD, suggesting that investigational drugs that engage these biomarkers as therapeutic targets may demonstrate comparable effects in both disorders.

Nonetheless, ADAD and LOAD are not identical. In addition to the relative over-production of $A\beta_{42}$ in ADAD and the effects of age and age-associated co-pathologies in LOAD, ADAD may generate unique cerebral biochemical changes. Specifically, *PSEN1* and *PSEN2* pathogenic variants alter the function of γ-secretase, a membrane-bound protease complex that includes the presenilin protein.[61] In conjunction with β-secretase, γ-secretase not only hydrolyses amyloid precursor protein (APP) to yield Aβ isoforms but also has >85 non-APP substrates, including molecules involved in signalling receptors and cell fate determination (e.g. Notch1).[62] Altered proteolytic degradation of these substrates by different *PSEN* pathogenic variants may result in peptide heterogeneity and biochemical diversity that in turn may contribute to variability in the number and distribution of amyloid deposits.[63] It has been suggested that such alterations may contribute to the greater symptomatic disease severity in ADAD as compared with LOAD;[64] another potential factor in the more aggressive symptomatic course may be that greater amyloid burden characterizes ADAD. However, young onset Alzheimer's disease without known pathogenic variants and thus lacking aberrant *PSEN* proteolytic

degradation also is characterized by a more aggressive course than LOAD, at least as measured by clinical features[65] and rates of cognitive decline,[66] and has greater neocortical tau aggregation than is observed in LOAD.[67]

Both ADAD and LOAD demonstrate heterogeneity. Although there are no obvious genotype-phenotype correlation in ADAD for clinical features[68] or for CSF $A\beta_{42}$, tau or p-tau_{181},[69] the mean age at symptomatic onset in ADAD is later for carriers of *APP* pathogenic variants (mean = 50.4 years, ±SD of 5.2 years) versus those with *PSEN1* pathogenic variants (mean = 43.6 years, ±7.2 years); also, *PSEN1* MCs with mutations before codon 200 have a younger age at onset (mean = 41.3 years, ±7.2 years) than those with mutations after codon 200 (mean = 45.8 years, ±6.4 years).[70] Several neuropathological and neuroimaging reports note elevated cerebral Aβ burden in ADAD individuals compared with those with LOAD[16,71–73]; one of these reports noted differences in the degree of amyloid angiopathy in *PSEN1* MCs with mutations before codon 200 compared with those with mutations after codon 200.[16] Despite similar functional decline, ADAD pathogenic variants show heterogeneity in Aβ burden as measured by PET PiB.[74] Although overall Aβ burden (plaques and amyloid angiopathy) was increased in a study of ADAD brains compared with LOAD brains, there were no differences in the densities of neuritic plaques and neurofibrillary tangles, nor were there differences in the degree of neuronal loss.[18] Synucleinopathy occurs in 42–50% of brains from both ADAD and LOAD; LOAD brains also demonstrate TDP-43 proteinopathy, argyrophilic grain disease, hippocampal sclerosis and infarcts.[14,15] The age at symptomatic onset in ADAD ranges from the third to the eighth decade of life[75,76] and even in the same pedigree can vary by over 30 years.[77] Persons entered into the National Alzheimer's Coordinating Center database (www.alz.washington.edu) with a diagnosis of sporadic Alzheimer's disease also demonstrate a wide range of age at diagnosis ranging from 36 to 104 years. The younger the age at symptomatic onset in LOAD, the more likely that the presenting feature is non-amnestic and the greater the frequency of behavioural symptoms, such as depression and apathy.[78] Atypical presentations of Alzheimer's disease are reported more often in LOAD[79,80] than in ADAD.[77] Features such as myoclonus, seizures and parkinsonism occur in both ADAD and LOAD, especially with longer disease durations[81] and with specific *PSEN1* pathogenic variants.[70] Spastic paraparesis is observed with some *PSEN1* pathogenic variants in ADAD[82]; the histopathological correlate of spastic paraparesis, 'cotton wool' plaques, occurs in both ADAD and LOAD.[83] Amyloid imaging has identified early striatal uptake in some *PSEN1* MCs.[84]

This study has limitations. The disparate ages of the cohorts, which may result in age-related confounding, required anchoring the cohorts on clinical disease progression; the anchor point for some individuals in both cohorts required estimation. The number of ADNI CDR 0 participants who subsequently progressed to CDR-SB ≥ 1 was small and the period of observation prior to symptomatic onset was brief. Both the DIAN and ADNI protocols changed over time, creating analytic challenges (e.g. need for CL conversion to reconcile PET data obtained with both PiB and florbetapir). The current study was initiated prior to the availability of newer molecular biomarkers, including tau PET, CSF markers of tau phosphorylated at position 217, synaptic integrity (e.g. SNAP-25; neurogranin) and axonal damage (e.g. neurofilament light), and plasma assays for $A\beta_{42}$, $A\beta_{40}$, p-tau isoforms and other markers. Finally, the small sample sizes for carriers of *APP* and *PSEN2* mutations limit the interpretation of possible gene- and mutation-specific effects on biomarkers and preclude a gene-specific comparison with LOAD on the biomarkers before and after symptomatic onset.

Although as yet unknown mechanisms may precede Aβ dysregulation, current data indicate that the initial pathophysiological event for both ADAD and LOAD is the disruption of Aβ homeostasis that produces in each a cascade of subsequent pathological events, including tauopathy and neurodegeneration, and ultimately results in the clinical expression of Alzheimer's disease. The unique dataset described in this report features by far the largest sample of ADAD MCs to undergo comprehensive baseline and longitudinal multimodal molecular biomarker studies. The comparison with LOAD was facilitated by the rigorous reprocessing of imaging data and CSF samples on uniform pipelines and platforms. The rates of change of molecular biomarkers for amyloid accumulation and tauopathy show no significant differences between ADAD and LOAD except that there may be greater amyloid accumulation as measured by CL in ADAD compared with LOAD after symptomatic onset. Thus, ADAD and LOAD have a similar pathophysiology as described by rates of changes for these molecular biomarkers of AD. Although ADAD has a more aggressive course after symptomatic onset than LOAD, as reflected by increased rates of change for cognitive decline and hippocampal volume loss, this faster rate of decline may permit earlier detection of any therapeutic effect in clinical trials with ADAD MCs. Our findings cannot assure that results from clinical trials of investigational anti-Alzheimer's disease drugs in the DIAN cohort can be extrapolated to LOAD, but they provide pathobiological support that such extrapolation is possible.

Acknowledgements

We thank all participants for their contribution to this research, and also thank DIAN and ADNI investigators and staff for their acquisition of the data, images and samples.

Funding

The comparison of ADAD and LOAD by reprocessing and analyzing existing data, images, and CSF was supported by a grant from the Alzheimer's Association (DIAN_ADNI-16-434364) and from an anonymous foundation.

DIAN data/image/tissue collection and sharing was supported by the Dominantly Inherited Alzheimer Network (DIAN, U19AG032438) funded by the National Institute on Aging (NIA), the German Center for Neurodegenerative Diseases (DZNE), Institute for Neurological Research (FLENI), the Research and Development Grants for Dementia from Japan Agency for Medical Research and Development, AMED NP21dk0207049 and NIHR UCL/UCLH Biomedical Research Centre and the MRC Dementias Platform UK (MR/L023784/1 and MR/009076/1).

Data collection and sharing for this project was funded by the Alzheimer's Disease Neuroimaging Initiative (ADNI) (National Institutes of Health Grant U01 AG024904) and DOD ADNI (Department of Defense award number W81XWH-12-2-0012). ADNI is funded by the National Institute on Aging, the National Institute of Biomedical Imaging and Bioengineering, and through generous contributions from the following: AbbVie, Alzheimer's Association; Alzheimer's Drug Discovery Foundation; Araclon Biotech; BioClinica, Inc.; Biogen; Bristol-Myers Squibb Company; CereSpir, Inc.; Cogstate; Eisai Inc.; Elan Pharmaceuticals, Inc.; Eli Lilly and Company; EuroImmun; F. Hoffmann-La Roche Ltd and

its affiliated company Genentech, Inc.; Fujirebio; GE Healthcare; IXICO Ltd.; Janssen Alzheimer Immunotherapy Research and Development, LLC.; Johnson and Johnson Pharmaceutical Research and Development LLC.; Lumosity; Lundbeck; Merck and Co., Inc.; Meso Scale Diagnostics, LLC.; NeuroRx Research; Neurotrack Technologies; Novartis Pharmaceuticals Corporation; Pfizer Inc.; Piramal Imaging; Servier; Takeda Pharmaceutical Company; and Transition Therapeutics. The Canadian Institutes of Health Research is providing funds to support ADNI clinical sites in Canada. Private sector contributions are facilitated by the Foundation for the National Institutes of Health (www.fnih.org). The grantee organization is the Northern California Institute for Research and Education, and the study is coordinated by the Alzheimer's Therapeutic Research Institute at the University of Southern California. ADNI data are disseminated by the Laboratory for Neuro Imaging at the University of Southern California.

This manuscript has been reviewed by DIAN Study investigators for scientific content and consistency of data interpretation with previous DIAN Study publications.

Competing interests

The authors report no competing interests.

Supplementary material

Supplementary material is available at *Brain* online.

References

1. Muller U, Winter P, Graeber MB. A presenilin 1 mutation in the first case of Alzheimer's disease. *Lancet Neurol*. 2013;12:129–130.
2. Rupp C, Beyreuther K, Maurer K, Kins S. A presenilin 1 mutation in the first case of Alzheimer's disease: Revisited. *Alzheimers Dement*. 2014;10:869–872.
3. Holtzman DM, Morris JC, Goate AM. Alzheimer's disease: The challenge of the second century. *Sci Transl Med*. 2011;3:77sr71.
4. Schenk D, Barbour R, Dunn W, *et al*. Immunization with amyloid-β attenuates Alzheimer-disease-like pathology in the PDAPP mouse. *Nature*. 1999;400:173–177.
5. Sperling RA, Rentz DM, Johnson KA, *et al*. The A4 study: Stopping AD before symptoms begin? *Sci Transl Med*. 2014;6:228fs213.
6. Bateman RJ, Benzinger TL, Berry S, *et al*. The DIAN-TU Next Generation Alzheimer's prevention trial: Adaptive design and disease progression model. *Alzheimers Dement*. 2017;13:8–19.
7. Reiman EM, Langbaum JB, Fleisher AS, *et al*. Alzheimer's prevention initiative: A plan to accelerate the evauation of presymptomatic treatments. *J Alzheimer Dis*. 2011;26:321–329.
8. Moulder KL, Snider BJ, Mills SL, *et al*. Dominantly inherited Alzheimer network: Facilitating research and clinical trials. *Alzheimers Res Ther*. 2013;5:48.
9. Patterson BW, Elbert DL, Mawuenyega KG, *et al*. Age and amyloid effects on human CNS amyloid-beta kinetics. *Ann Neurol*. 2015;78:439–453.
10. Potter R, Patterson BW, Elbert DL, *et al*. Increased in vivo amyloid-β42 production, exchange, and loss in presenilin mutation carriers. *Sci Transl Med*. 2013;5:189ra177.
11. Lopera F, Ardilla A, Martinez A, *et al*. Clinical features of early-onset Alzheimer disease in a large kindred with an E280A presenilin-1 mutation. *JAMA*. 1997;277:793–799.
12. Ryman DC, Acosta-Baena N, Aisen PS, *et al*. Symptom onset in autosomal dominant Alzheimer disease: A systematic review and meta-analysis. *Neurology*. 2014;83:253–260.
13. Global, regional, and national burden of neurological disorders, 1990-2016: A systematic analysis for the Global Burden of Disease Study 2016. *Lancet Neurol*. 2019;18:459–480.
14. Boyle PA, Yu L, Wilson RS, Leurgans SE, Schneider JA, Bennett DA. Person-specific contribution of neuropathologies to cognitive loss in old age. *Ann Neurol*. 2018;83:74–83.
15. Cairns NJ, Perrin RJ, Franklin EE, *et al*. Neuropathologic assessment of participants in two multi-center longitudinal observational studies: The Alzheimer Disease Neuroimaging Initiative (ADNI) and the Dominantly Inherited Alzheimer Network (DIAN). *Neuropathology*. 2015;35:390–400.
16. Mann DM, Pickering-Brown SM, Takeuchi A, Iwatsubo T. Amyloid angiopathy and variability in amyloid beta deposition is determined by mutation position in presenilin-1-linked Alzheimer's disease. *Am J Pathol*. 2001;158:2165–2175.
17. Day GS, Musiek ES, Roe CM, *et al*. Phenotypic Similarities between late-onset autosomal dominant and sporadic Alzheimer disease: A single-family case-control study. *JAMA Neurol*. 2016;73:1125–1132.
18. Lippa CF, Saunders AM, Smith TW, *et al*. Familial and sporadic Alzheimer's disease: Neuropathology cannot exclude a final common pathway. *Neurology*. 1996;46:406–412.
19. Falcon B, Zhang W, Schweighauser M, *et al*. Tau filaments from multiple cases of sporadic and inherited Alzheimer's disease adopt a common fold. *Acta Neuropathol*. 2018;136:699–708.
20. Salloway S, Farlow M, McDade E, *et al*. A trial of gantenerumab or solanezumab in dominantly inherited Alzheimer's disease. *Nat Med*. 2021;27:1187–1196.
21. Aisen PS, Zhou J, Irizarry MC, *et al*. AHEAD 3-45 study design: A global study to evaluate the efficacy and safety of treatment with BAN2401 for 216 weeks in preclinical Alzheimer's disease with intermediate amyloid (A3 trial) and elevated amyloid (A45 trial). *Alzheimers Dement*. 2020;16:e044511.
22. Mintun MA, Lo AC, Duggan Evans C, *et al*. Donanemab in early Alzheimer's disease. *N Engl J Med*. 2021;384:1691–1704.
23. Swanson CJ, Zhang Y, Dhadda S, *et al*. A randomized, double-blind, phase 2b proof-of-concept clinical trial in early Alzheimer's disease with lecanemab, an anti-Aβ protofibril antibody. *Alzheimers Res Ther*. 2021;13:80.
24. Morris JC, Aisen PS, Bateman RJ, *et al*. Developing an international network for Alzheimer's research: The Dominantly Inherited Alzheimer Network. *Clin Investig*. 2012;2:975–984.
25. Natté R, Maat-Schieman ML, Haan J, Bornebroek M, Roos RA, van Duinen SG. Dementia in hereditary cerebral hemorrhage with amyloidosis-Dutch type is associated with cerebral amyloid angiopathy but is independent of plaques and neurofibrillary tangles. *Ann Neurol*. 2001;50:765–772.
26. Morris JC, Weintraub S, Chui HC, *et al*. The Uniform Data Set (UDS): Clinical and cognitive variables and descriptive data from Alzheimer Disease Centers. *Alzheimer Dis Assoc Disord*. 2006;20:210–216.
27. Weintraub S, Salmon D, Mercaldo N, *et al*. The Alzheimer's Disease Centers' Uniform Data Set (UDS): The neuropsychologic test battery. *Alzheimer Dis Assoc Disord*. 2009;23:91–101.
28. Morris JC. The Clinical Dementia Rating (CDR): Current version and scoring rules. *Neurology*. 1993;43:2412–2414.
29. Berg L, Miller JP, Storandt M, *et al*. Mild senile dementia of the Alzheimer type: 2. Longitudinal assessment. *Ann Neurol*. 1988;23:477–484.
30. Mueller SG, Weiner MW, Thal LJ, *et al*. The Alzheimer's disease neuroimaging initiative. *Neuroimaging Clin N Am*. 2005;15:869–877, xi-xii.

31. Petersen RC, Aisen PS, Beckett LA, *et al*. Alzheimer's Disease Neuroimaging Initiative (ADNI): Clinical characterization. *Neurology*. 2010;74:201–209.
32. Sheikh JI, Yesavage JA, eds. Geriatric Depression Scale (GDS): Recent evidence and development of a shorter version. In: *Clinical gerontology: A guide to assessment and intervention*. New York: The Haworth Press; 1986:165–173.
33. Day GS, Long A, Morris JC. Assessing the reliability of reported medical history in older adults. *J Alzheimers Dis*. 2020;78:643–652.
34. Beach TG, Monsell SE, Phillips LE, Kukull W. Accuracy of the clinical diagnosis of Alzheimer disease at National Institute on Aging Alzheimer Disease Centers, 2005-2010. *J Neuropathol Exp Neurol*. 2012;71:266–273.
35. Langa KM, Levine DA. The diagnosis and management of mild cognitive impairment: a clinical review. *JAMA*. 2014;312:2551–2561.
36. Bateman RJ, Xiong C, Benzinger TL, *et al*. Clinical and biomarker changes in dominantly inherited Alzheimer's disease. *N Engl J Med*. 2012;367:795–804.
37. Saykin AJ, Shen L, Yao X, *et al*. Genetic studies of quantitative MCI and AD phenotypes in ADNI: Progress, opportunities, and plans. *Alzheimers Dement*. 2015;11:792–814.
38. Hansson O, Seibyl J, Stomrud E, *et al*. CSF biomarkers of Alzheimer's disease concord with amyloid-β PET and predict clinical progression: A study of fully automated immunoassays in BioFINDER and ADNI cohorts. *Alzheimers Dement*. 2018;14:1470–1481.
39. Hansson O, Lehmann S, Otto M, Zetterberg H, Lewczuk P. Advantages and disadvantages of the use of the CSF Amyloid β (Aβ) 42/40 ratio in the diagnosis of Alzheimer's disease. *Alzheimers Res Ther*. 2019;11:34.
40. Korecka M, Figurski MJ, Landau SM, *et al*. Analytical and clinical performance of amyloid-beta peptides measurements in CSF of ADNIGO/2 participants by an LC-MS/MS reference method. *Clin Chem*. 2020;66:587–597.
41. Jack CR, Jr, Lowe VJ, Senjem ML, *et al*. 11C PiB and structural MRI provide complementary information in imaging of Alzheimer's disease and amnestic mild cognitive impairment. *Brain*. 2008;131:665–680.
42. Fischl B. FreeSurfer. *Neuroimage*. 2012;62:774–781.
43. Fischl B, van der Kouwe A, Destrieux C, *et al*. Automatically parcellating the human cerebral cortex. *Cereb Cortex*. 2004;14:11–22.
44. Buckner RL, Head D, Parker J, *et al*. A unified approach for morphometric and functional data analysis in young, old, and demented adults using automated atlas-based head size normalization: Reliability and validation against manual measurement of total intracranial volume. *Neuroimage*. 2004;23:724–738.
45. Dincer A, Gordon BA, Hari-Raj A, *et al*. Comparing cortical signatures of atrophy between late-onset and autosomal dominant Alzheimer disease. *Neuroimage Clin*. 2020;28:102491.
46. Su Y, D'Angelo GM, Vlassenko AG, *et al*. Quantitative analysis of PiB-PET with FreeSurfer ROIs. *PLoS ONE*. 2013;8:e73377.
47. Su Y, Flores S, Wang G, *et al*. Comparison of Pittsburgh compound B and florbetapir in cross-sectional and longitudinal studies. *Alzheimers Dement*. 2019;11:180–190.
48. Jagust WJ, Landau SM, Koeppe RA, *et al*. The Alzheimer's Disease Neuroimaging Initiative 2 PET Core: 2015. *Alzheimers Dement*. 2015;11:757–771.
49. Gordon BA, Blazey TM, Su Y, *et al*. Spatial patterns of neuroimaging biomarker change in individuals from families with autosomal dominant Alzheimer's disease: A longitudinal study. *Lancet Neurol*. 2018;17:241–250.
50. Su Y, Blazey TM, Snyder AZ, *et al*. Partial volume correction in quantitative amyloid imaging. *Neuroimage*. 2015;107:55–64.
51. Rousset OG, Ma Y, Evans AC. Correction for partial volume effects in PET: Principle and validation. *J Nucl Med*. 1998;39:904–911.
52. Klunk WE, Koeppe RA, Price JC, *et al*. The Centiloid Project: Standardizing quantitative amyloid plaque estimation by PET. *Alzheimers Dement*. 2015;11:1–15.e11-14.
53. Su Y, Flores S, Hornbeck RC, *et al*. Utilizing the Centiloid scale in cross-sectional and longitudinal PiB PET studies. *NeuroImage Clinical*. 2018;19:406–416.
54. Laird NM, Ware JH. Random-effects models for longitudinal data. *Biometrics*. 1982;38:963–974.
55. *SAS/STAT software, Version 9.4 (TS1M6) for Windows*. Cary, NC, 2016.
56. Fotenos AF, Mintun MA, Snyder AZ, Morris JC, Buckner RL. Brain volume decline in aging: evidence for a relationship between socioeconomic status, preclinical Alzheimer's disease, and reserve. *Arch Neurol*. 2008;65:113–120.
57. Schippling S, Ostwaldt AC, Suppa P, *et al*. Global and regional annual brain volume loss rates in physiological aging. *J Neurol*. 2017;264:520–528.
58. Buckles VD, Xiong C, Bateman RJ, *et al*. Different rates of cognitive decline in autosomal dominant and late-onset Alzheimer disease. *Alzheimers Dement*. Published online 2 December 2021. doi:10.1002/alz.12505
59. Jack CR, Jr, Bennett DA, Blennow K, *et al*. NIA-AA Research Framework: Toward a biological definition of Alzheimer's disease. *Alzheimers Dement*. 2018;14:535–562.
60. Ebenau JL, Pelkmans W, Verberk IMW, *et al*. Association of CSF, plasma, and imaging markers of neurodegeneration with clinical progression in people with subjective cognitive decline. *Neurology*. 2022;98:e1315–e1326.
61. Kimberly WT, LaVoie MJ, Ostaszewski BL, Ye W, Wolfe MS, Selkoe DJ. Gamma-secretase is a membrane protein complex comprised of presenilin, nicastrin, Aph-1, and Pen-2. *Proc Natl Acad Sci USA*. 2003;100:6382–6387.
62. Haapasalo A, Kovacs DM. The many substrates of presenilin/γ-secretase. *J Alzheimers Dis*. 2011;25:3–28.
63. Maarouf CL, Daugs ID, Spina S, *et al*. Histopathological and molecular heterogeneity among individuals with dementia associated with Presenilin mutations. *Mol Neurodegener*. 2008;3:20.
64. Roher AE, Maarouf CL, Kokjohn TA. Familial presenilin mutations and sporadic Alzheimer's disease pathology: Is the assumption of biochemical equivalence justified? *J Alzheimers Dis*. 2016;50:645–658.
65. Seltzer B, Sherwin I. A comparison of clinical features in early- and late-onset primary degenerative dementia. One entity or two? *Arch Neurol*. 1983;40:143–146.
66. van der Vlies AE, Koedam EL, Pijnenburg YA, Twisk JW, Scheltens P, van der Flier WM. Most rapid cognitive decline in APOE epsilon4 negative Alzheimer's disease with early onset. *Psychol Med*. 2009;39:1907–1911.
67. Schöll M, Ossenkoppele R, Strandberg O, *et al*. Distinct 18F-AV-1451 tau PET retention patterns in early- and late-onset Alzheimer's disease. *Brain*. 2017;140:2286–2294.
68. Larner AJ. Presenilin-1 mutations in Alzheimer's disease: An update on genotype-phenotype relationships. *J Alzheimers Dis*. 2013;37:653–659.
69. Wallon D, Rousseau S, Rovelet-Lecrux A, *et al*. The French series of autosomal dominant early onset Alzheimer's disease cases:

mutation spectrum and cerebrospinal fluid biomarkers. *J Alzheimers Dis*. 2012;30:847–856.
70. Ryan NS, Nicholas JM, Weston PSJ, *et al*. Clinical phenotype and genetic associations in autosomal dominant familial Alzheimer's disease: A case series. *Lancet Neurol*. 2016;15:1326–1335.
71. Gomez-Isla T, Growdon WB, McNamara MJ, *et al*. The impact of different presenilin 1 andpresenilin 2 mutations on amyloid deposition, neurofibrillary changes and neuronal loss in the familial Alzheimer's disease brain: evidence for other phenotype-modifying factors. *Brain*. 1999;122:1709–1719.
72. Shepherd C, McCann H, Halliday GM. Variations in the neuropathology of familial Alzheimer's disease. *Acta Neuropathol*. 2009;118:37–52.
73. Ryan NS, Biessels GJ, Kim L, *et al*. Genetic determinants of white matter hyperintensities and amyloid angiopathy in familial Alzheimer's disease. *Neurobiol Aging*. 2015;36:3140–3151.
74. Chhatwal JP, Schultz SA, McDade E, *et al*. Variant-dependent heterogeneity in amyloid β burden in autosomal dominant Alzheimer's disease: Cross-sectional and longitudinal analyses of an observational study. *Lancet Neurol*. 2022;21:140–152.
75. Snider BJ, Norton J, Coats MA, *et al*. Novel presenilin 1 mutation (S170F) causing Alzheimer disease with Lewy bodies in the third decade of life. *Arch Neurol*. 2005;62:1821–1830.
76. Jayadev S, Leverenz JB, Steinbart E, *et al*. Alzheimer's disease phenotypes and genotypes associated with mutations in presenilin 2. *Brain*. 2010;133:1143–1154.
77. Larner AJ, Doran M. Clinical phenotypic heterogeneity of Alzheimer's disease associated with mutations of the presenilin-1 gene. *J Neurol*. 2006;253:139–158.
78. Barnes J, Dickerson BC, Frost C, Jiskoot LC, Wolk D, van der Flier WM. Alzheimer's disease first symptoms are age dependent: Evidence from the NACC dataset. *Alzheimers Dement*. 2015;11:1349–1357.
79. Galton CJ, Patterson K, Xuereb JH, Hodges JR. Atypical and typical presentations of Alzheimer's disease: A clinical, neuropsychological, neuroimaging and pathological study of 13 cases. *Brain*. 2000;123:484–498.
80. Lam B, Masellis M, Freedman M, Stuss DT, Black SE. Clinical, imaging, and pathological heterogeneity of the Alzheimer's disease syndrome. *Alzheimers Res Ther*. 2013;5:1.
81. Chen JY, Stern Y, Sano M, Mayeux R. Cumulative risks of developing extrapyramidal signs, psychosis, or myoclonus in the course of Alzheimer's disease. *Arch Neurol*. 1991;48:1141–1143.
82. Crook R, Verkkoniemi A, Perez-Tur J, *et al*. A variant of Alzheimer's disease with spastic paraparesis and unusual plaques due to deletion of exon 9 of presenilin 1. *Nat Med*. 1998;4:452–455.
83. Le TV, Crook R, Hardy J, Dickson DW. Cotton wool plaques in non-familial late-onset Alzheimer disease. *J Neuropathol Exp Neurol*. 2001;60:1051–1061.
84. Klunk WE, Price JC, Mathis CA, *et al*. Amyloid deposition begins in the striatum of presenilin-1 mutation carriers from two unrelated pedigrees. *J Neurosci*. 2007;27:6174–6184.